JCHR (2024) 14(4), 867-879

Journal of Chemical Health Risks

sanad.iau.ir/journal/jchr

ORIGINAL ARTICLE

Investigation ZnO and Different Additives on Ultrasonic Degradation of Bisphenol A

Shaharul Islam[*1, 2], Samiul Bari Avick[1], M. Shamsul Alam[1], Helal Uddin[*1]

[1]*Department of Applied Chemistry and Chemical Engineering, Faculty of Engineering and Technology, Islamic University, Kushtia-7003, Bangladesh*

[2]*Department of Chemistry, Bangladesh Army University of Engineering & Technology (BAUET), Qadirabad Cantonment, Natore-6431, Bangladesh*

(Received: 16 February 2024 Accepted: 6 July 2024)

KEYWORDS
Bisphenol A;
Ultrasound;
Degradation;
Nanoparticles;
Additives

ABSTRACT: Degradation of bisphenol A (BPA) or 4, 4'-isopropylidene diphenol, a common endocrine disruptor was carried out by ultrasound irradiation at 40 kHz in the presence of ZnO nanoparticles, NaCl, Na_2SO_4, H_2O_2, and CCl_4. The BPA degradation is carried out at pH 6.3(stock solution), pH 2, and 8 in the presence and absence of the aforesaid additives at different concentrations. The degradation behavior of BPA was measured through the UV-visible spectrophotometer. The ZnO nanoparticle was synthesized by the Sol-Gel method and characterized by SEM, EDX, and XRD. The experimental result shows that the rate of degradation increased with the addition of additives. The synthesized ZnO nanoparticle drastically favored the degradation rate of BPA. The BPA degradation rate is also improved in acidic conditions compared to the basic conditions. Therefore, the BPA can be efficiently removed from the aqueous medium using ultrasound irradiation in the presence of ZnO nanoparticles, NaCl, Na_2SO_4, H_2O_2, and CCl_4.

INTRODUCTION

Phenols include TBP group substances i.e. toxic, bioaccumulative, and persevering in environmental matrix compounds. One of these phenols, known as bisphenol A (4,4'-isopropylidene diphenol or BPA), is commonly found in surface waters and wastewater. It serves as a monomer for a variety of plastics [1]. The breakdown of endocrine-disrupting chemicals (EDCs) is a crucial topic for maintaining our ecosystem in the long run. Known to have a potent estrogenic endocrine disrupting impact, BPA is a common EDC that also causes a several illnesses, including carcinogenesis [2-4]. BPA is harmful to animal and human health [5-8]. At different phases of human life, such as the fetal, childhood, and adult stages, this influences the enzymatic, neurological, androgenic, hepatic, and reproductive systems [9, 10]. Despite its mild severe toxicity, it has a female hormone impact. DNA binding results from BPA's metabolic activation [11]. BPA was found in surface water contaminated by industrial wastewater discharges by Matsumoto et al. and Matsumoto [12, 13]. Environmental experts concerned about BPA pollution of water have been looking for efficient ways to destroy EDCs because they are a persistent chemical to break down. Modern chemical oxidation treatment techniques can potentially cure any kind of organic or inorganic pollutant, regardless of whether it is volatile, semivolatile, or nonvolatile. Most commonly, these oxygen-based processes are referred to

*Corresponding author: shaharul.acct@gmail.com; uddindrhelal@gmail.com (Sh. Islam; Helal Uddin)
DOI: 10.60829/jchr.2024.92351

as Advanced Oxidation Processes (AOPs). All things considered, an oxidation process that produces enough hydroxyl radicals to influence any form of chemical reaction is known as an AOP. Advanced oxidation technologies are considered a rapid development in the field of environmental sonochemistry [14–21]. Cavitation, the violent collapse of bubbles, allows for this method; the temperature inside the cavitation can reach several thousand degrees. Every acoustic cycle produces OH radicals because the bubble contains water vapor. Water molecules break down to generate extremely reactive radical such as hydrogen, hydroperoxide, and hydroxyl radicals. These can oxidize organic materials and damage the pollutant's molecular structure, leading to the degrading effect [22, 23]. Radicals with a high potential for oxidation target organic contaminants, resulting in the formation of smaller molecular weight molecules [24]. Strong pressure waves are also produced when collapsing bubbles implode, and these waves are employed in wastewater treatment systems for both chemical and physical processes [24]. Equations 1-6 indicate that the following reactive radicals are generated by the phenomenon of ultrasonic cavitation [25]:

$$H_2O + \text{ultrasound} \rightarrow \bullet OH + H\bullet \quad (1)$$

$$O_2 + \text{ultrasound} \rightarrow 2O\bullet \quad (2)$$

$$H\bullet + O_2 \rightarrow \bullet OOH \quad (3)$$

$$O\bullet + H_2O \rightarrow 2\ \bullet OH \quad (4)$$

$$\bullet OH + \bullet OH \rightarrow H_2O_2 \quad (5)$$

$$H_2O_2 + \text{ultrasound} \rightarrow 2\bullet OH \quad (6)$$

These radicals appear at the interface between cavitation and water, where they react with solute molecules. This is particularly the case where the solute molecules are intense at the interface, as is the case with BPA.

$$\bullet OH + BPA \rightarrow \text{Products} \quad (7)$$

It should be mentioned that the degradation reaction frequently occurs as a pseudo-first-order reaction and that the concentration of OH may be effectively considered constant throughout the experiment's time range. BPA does not fall into the category of volatile solutes that can be immediately broken down by heat, a process similar to pyro chemistry, if the solute molecules are so volatile that they can enter the cavitation. One benefit of the sonochemical process is that it is a self-contained system that uses ultrasonic transducers and a power source at the right frequency. It also operates as long as there is electrical power available. The degradation of Phenolic compounds and dyes has been the subject of numerous researches [26 – 33]. Extensive study has been conducted on the development of effective additives to accelerate the breakdown of organic chemicals. Recent research has examined the effects of CCl_4 or C_6F_{14} additions on sonochemical degradation [33-35]. Even though CCl_4 is one of the more hazardous compounds and is therefore used under strict regulations, it is an effective addition to hasten the target organic molecules' sonochemical disintegration. The presence of 19 mg $L^{-1}C_6F_{14}$ boosted the rates at which phenol was removed from the olive mill's wastewater, according to Sponza et al. [34]. Zeng et al. reported that the sonolytic degradation of phenol increased from 0.014 to 0.031 min^{-1} or from 0.014 to 0.032 min^{-1}, respectively for 150 M CCl_4 or 1.5 M C_6F_{14}[35]. Based on research these advantageous effects are attributed to the H atom scavenger properties of CCl_4 or C_6F_{14} [34, 35]. Furthermore, it has been observed that the use of specific chemicals such as NaCl and Na_2SO_4 may impact the rate at which colors deteriorate [36-38]. However, a lot of study has been done on metal oxide semiconductors and their potential as photocatalysts to eliminate organic contaminants from air and water [39-42]. The active sites of electron-hole pairs are produced when the metal oxides are activated by the right amount of photon energy, and this increases the catalytic activity on the metal oxide surfaces [43]. Among these metal oxides, TiO_2 is thought to be the most ideal material due to its outstanding stability and relatively simple manufacturing technique [44–47]. Zinc oxide (ZnO) with an exciton binding energy of 60 m eV and a rather broad band gap of 3.37 eV, has been widely studied as a photocatalyst for the degradation of various organic pollutants. Moreover, ZnO nanostructures are preferred over TiO_2 as photocatalyst alternatives for photodegradation due to their more favorable solar spectrum absorption, affordability, and nontoxicity [48]. In numerous studies, ZnO nanostructures demonstrated potent photocatalytic activity for the elimination of organic contaminants from such organic compounds [49]. Therefore, in this study, we have examined the

effects of ZnO nanoparticles, NaCl, Na_2SO_4, H_2O_2, and CCl_4 on the sonolytic degradation of BPA. Furthermore, to maximize the sonochemical breakdown rate of BPA in water, we have studied several factors, including pH, and additive concentration (ZnO nanoparticles, NaCl, Na_2SO_4, H_2O_2, and CCl_4).

MATERIALS AND METHODS

Materials and equipments

BPA or 4,4'-isopropylidenediphenol ($C_{15}H_{16}O_2$), Merck Life Science, Godraj One, 8th Floor, piroj sha nagar, Vadhroli East, Mumbai-400079, Sodium Chloride (NaCl), RANBAXY Fine chemicals Lt. A-3, Okhla industrial area, phase-l, New Delhi-l10020 (ISO 9001: 2000 certified company), Sodium sulfate (Na_2SO_4), Merck Specialities Private Limited, Shiv Sagor Estate `A` Dr Annic Besant Road, Worli, Mumbai-400018, Hydrogen peroxide (H_2O_2), Merck KGaA, 64271 Darmstadt, Germany, Carbon tetrachloride (CCI_4), Merck, D-6100 Darmstadt, FR. Germany. All of the chemicals were analytical grade and used without further purification. The model of the Sonicator used in this study was YZ5120-1(China) with 120 W powers and the UV spectrophotometer model was Shimadzu UV-1900I. In all experiments, we have followed the Standards Operating Procedures (SOPs) and Analytical Quality Assurance standards.

Preparation of solutions

BPA solutions containing $25mgl^{-1}$ were prepared. The inorganic salts NaCl and Na_2SO_4 were dissolved in 100 milliliters of distilled water with 36 and 13.9 grams of salt, respectively, based on their maximum saturation values. One liter of distilled water has been mixed with 1.02 ml of H_2O_2 to produce 10 mMl^{-1} H_2O_2 solutions. Using a micro syringe, the 100 and 200 µl CCl_4 was adjusted.

Preparation of zinc oxide nanoparticles

Zinc oxide nanoparticles were prepared by using the Sol-Gel technique. 30g of $Zn(NO_3)_2$ were dissolved in 500 ml of demineralized water to generate $Zn(NO_3)_2$ solution. Five minutes of stirring was needed for the solution. To make a KOH solution, dissolve 25 grams of KOH in 300 ml of demineralized water. It is also stirred for five minutes. The $Zn(NO_3)_2$ solution was vigorously stirred as the KOH solution was gradually added. After two hours of stirring the solution, a white precipitate of ZnO nanoparticle was developed. After that, the precipitate was centrifuged for fifteen minutes. After that, it was filtered. To remove the impurities, ethanol was used three times to wash the precipitate during filtration. Finally, demineralized water was used to wash it. After that, it was dried at 62^0C in an oven for 30 minutes. It was allowed to cool to ambient temperature after drying. After that, it was heated to 260°C for two hours in a furnace. Then it was placed to store for further usage after cooling at room temperature.

RESULTS AND DISCUSSION

Morphological and compositional characteristics of ZnO nano-particles

Multiple single diffraction peaks at 2θ angles are visible in the XRD pattern (Figure 1); these peaks correspond to different ZnO nanoparticle crystallographic planes. Mainly at 31.76°, 34.42°, 36.24°, 47.44°, 56.54°, 62.8°, 66.08°, 67.84°, and 68.14° are the detected diffraction peaks. The (100), (002), (101), (102), (110), (103), (200), (004), and (202) planes can be used to index these peaks. These planes resemble the ZnO hexagonal wurtzite crystal structure (JCPDS No. 80-0075). The fact that no other peaks belonging to contaminants or secondary phases were found supports the finding that pure ZnO nanoparticles were formed. The ZnO nanoparticles' crystalline size (D) was calculated using the Scherrer equation as follows:

$$D = k\lambda/\beta\cos(\theta) \qquad (8)$$

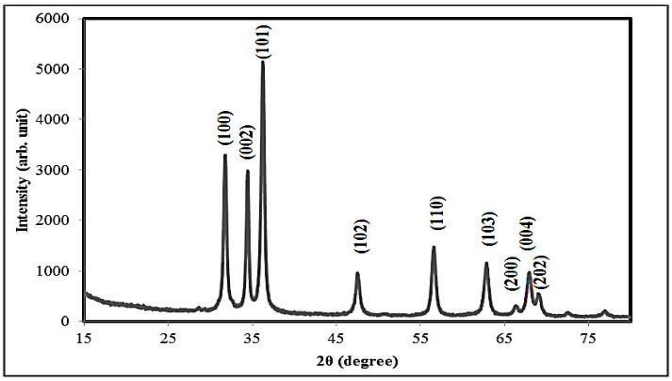

Figure 1. XRD pattern of prepared ZnO nanoparticles.

In this configuration, D stands for the crystalline size, λ for the X-ray radiation wavelength (Cu Kα, 1.5418 Å), k for the Scherrer constant (0.94), β for the full width at half maximum (FWHM) of the diffraction peak, and θ for the Bragg angle. The XRD peaks provided the FWHM values, which were then used to compute the corresponding crystalline sizes. According to Table 1, the average size of the crystal was found to be approximately 29.5981 nm, suggesting that ZnO nanoparticles were developing in the nanometer range.

Table 1. The estimated range of the structural properties of the synthesized ZnO nanoparticle.

Synthesized NPs	Position of Peak, (101) (2θ°)	Height of Peak, (arb unit.)	Size of Crystallite, (nm)	Microstrain, ε ($\times10^{-3}$)	Dislocation density, δ ($\times10^{-3}$ nm^{-2})
Pure ZnO	36.2547	5142	29.5981	0.4216	1.1414

Field emission scanning microscopy (FESEM) has been used to morphologically analyze the synthesized ZnO products. Figure 2 displays images captured by a FESEM of synthetic ZnO nanoparticles. The produced ZnO nanoparticles are formed at very high density with varied diameters, as shown in Figure 2(a). According to the high-magnification image in Figures 2(b) and 2(c), each ZnO nanoparticle is made up of particles that range in size from ~31 to ~61 nm on average.

To determine the element composition of produced ZnO nanoparticles, energy-dispersive X-ray spectroscopy (EDX) has been investigated. In the EDX spectrum shown in Figure 2(d), the only peaks are for zinc (79.79% by weight) and oxygen (20.21% by weight) with no contaminants visible. The ZnO nanoparticles produced through synthetic means are pure and exclusively contain zinc and oxygen which is confirmed again by EDX examination.

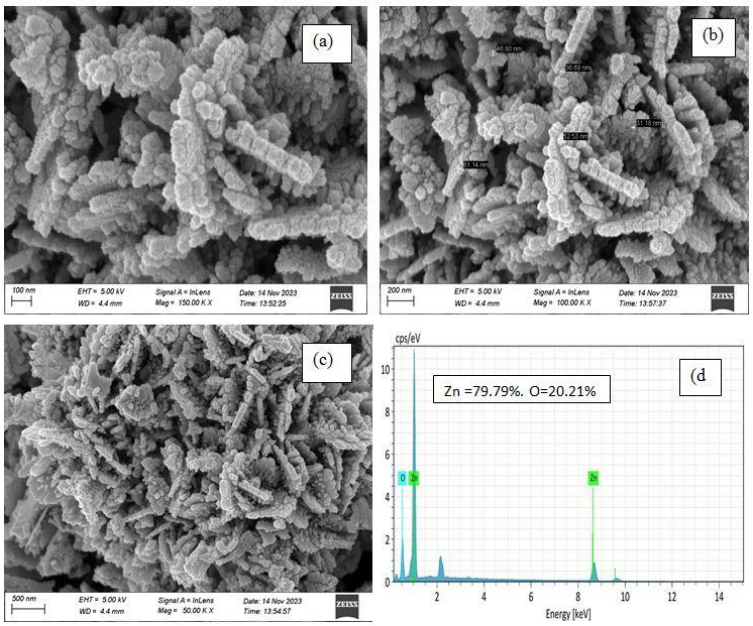

Figure 2. (a) Low, (b) medium, and (c) high magnification FESEM images, (d) EDX spectrum of synthesized ZnO nanoparticles.

Effect of pH on BPA degradation

The graph illustrates exponential curves shown as solid curves, derived from the model function of first-order kinetics.

$$x = ae^{-kt} \quad (9)$$

Where t is the degradation time, k is a fitting parameter that needs to be adjusted, and the constant "a" represents the primary concentration of BPA (25 mgl^{-1}). Below is a discussion and display of the BPA degradation rates under various conditions using sonochemical irradiation techniques, without the use of additives. Solutions of NaOH and H_2SO_4 have been used to maintain the solution pH.

In Figure 3 the sonolytic degradation of BPA at different pH are depicted. Following the figure it is clear that the degradation is improved with increasing sonication time. It is also found that the rate of degradation is increased with the lowering of the pH of pure BPA solution. The maximum degradation was obtained at pH 2 compared to the pH 8 and stock solution. The preliminary results indicate that BPA removal was primarily regulated by oxidation induced by the •OH radical, which is responsible for the lower BPA removal efficiency in alkaline solution and the higher BPA removal efficiency in acidic solution. The solvated electron from the water is readily transformed to H in an acidic solution by reacting with H^+, which inhibits the interaction with •OH and raises the concentration of the •OH radical in the solution. •OH radical may react with OH^- at a high rate constant in an alkaline solution, resulting in a drop in the concentration of •OH [50]. However, at high pH levels, ions produced by NaOH also competed with BPA for adsorption [51].

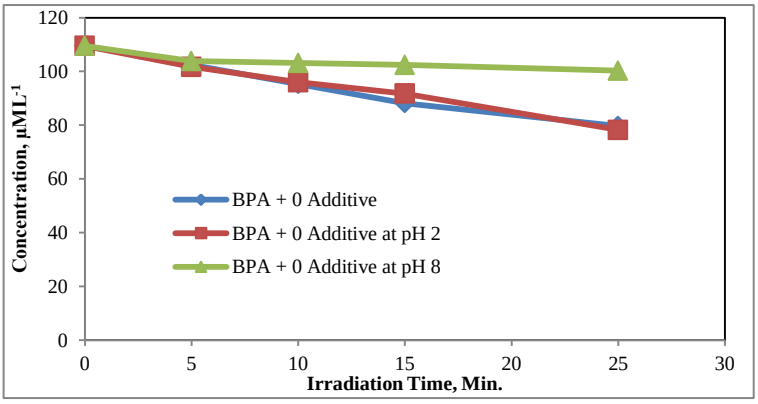

Figure 3. Sonochemical degradation of pure BPA at different pH.

Effect of ZnO on BPA Degradation

Sonolysis of BPA is carried out in the presence of the synthesized ZnO nanoparticle at pH 6.3(stock solution), pH 2, and pH 8. Figure 4 demonstrates the degradation rate of BPA with ZnO nanoparticles. It is observed that the BPA degradation rate is greatly improved as the sonication time increases and the highest degradation is obtained for ZnO in an acidic medium compared to others.

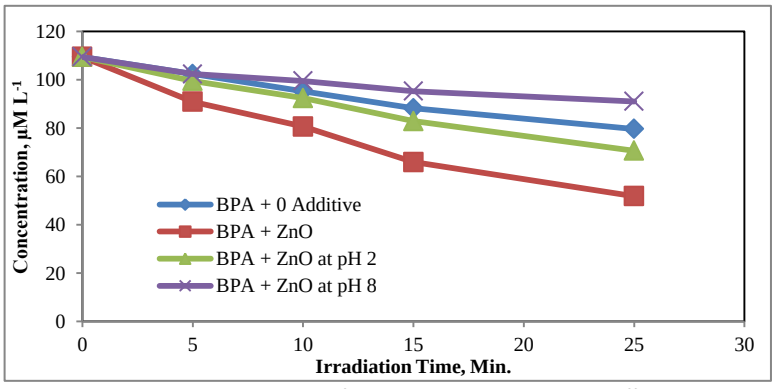

Figure 4. Sonochemical degradation of BPA with ZnO nanoparticles at different pH.

It is also noted from the experiment that the degradation is lowest for the basic conditions(at pH 8) and increased to the acidic conditions (at pH 2). A Study conducted by Sin et al. showed that the photocatalytic enhancement of ZnO was attributed to the OH generation ability and high charge separation efficiency [52]. Kamaraj et al. observed that synthesized ZnO-NPs showed greater photocatalytic affectivity of BPA under sunlight irradiation and near-complete mineralization of BPA which is agreed with our current study [53]. The highly crystalline structure of ZnO is aided the photoactivity and the porous structure is beneficial for the adsorption and degradation of BPA.

Effect of NaCl on BPA degradation

The degradation behavior of BPA under ultrasonic irradiation in the presence of NaCl is shown in Figure 5. The sonolysis is carried out for pure BPA, BPA with 10 ml NaCl, and BPA with 20 ml NaCl. The concentration of BPA decreased with the increased doses of NaCl and irradiation time(Figures 5a, 5b, and 5c). It is found that degradation for a stock solution with NaCl is higher than that of the solution at pH 2 and pH 8 i.e. the basic condition is unfavorable for the BPA degradation in the presence of NaCl. The reason for this is that the production of hypochlorite ions, chlorite ions, and other potent oxidation products through Cl^- reaction with OH radical has a significant impact on the degradation of BPA [54].

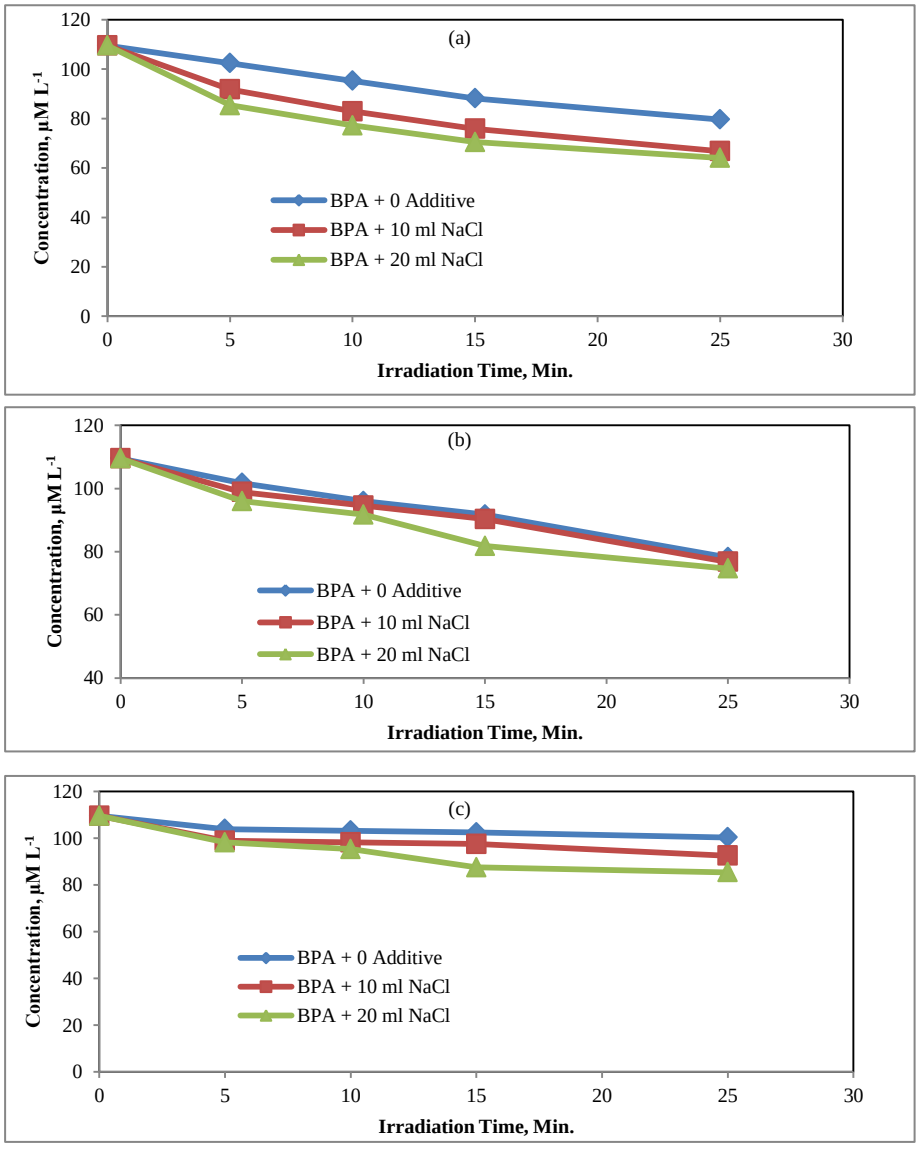

Figure 5. Sonochemical degradation of BPA, BPA with 10mL and 20mL NaCl at (a) pH = 6.3 (stock solution), (b) pH = 2, and (c) pH = 8.

Effect of Na_2SO_4 on BPA degradation

Degradation of BPA with different concentrations of Na_2SO_4 at three pH viz. 6.3, 2, and 8 are demonstrated in figure 6. From the result of sonolysis, we get that for the solution with pH 2(Figure 6b) 20 ml Na_2SO_4 enhances the degradation of BPA more effectively in comparison to the 10 ml Na_2SO_4 and without any additive. Figure 6a and 6c follow.

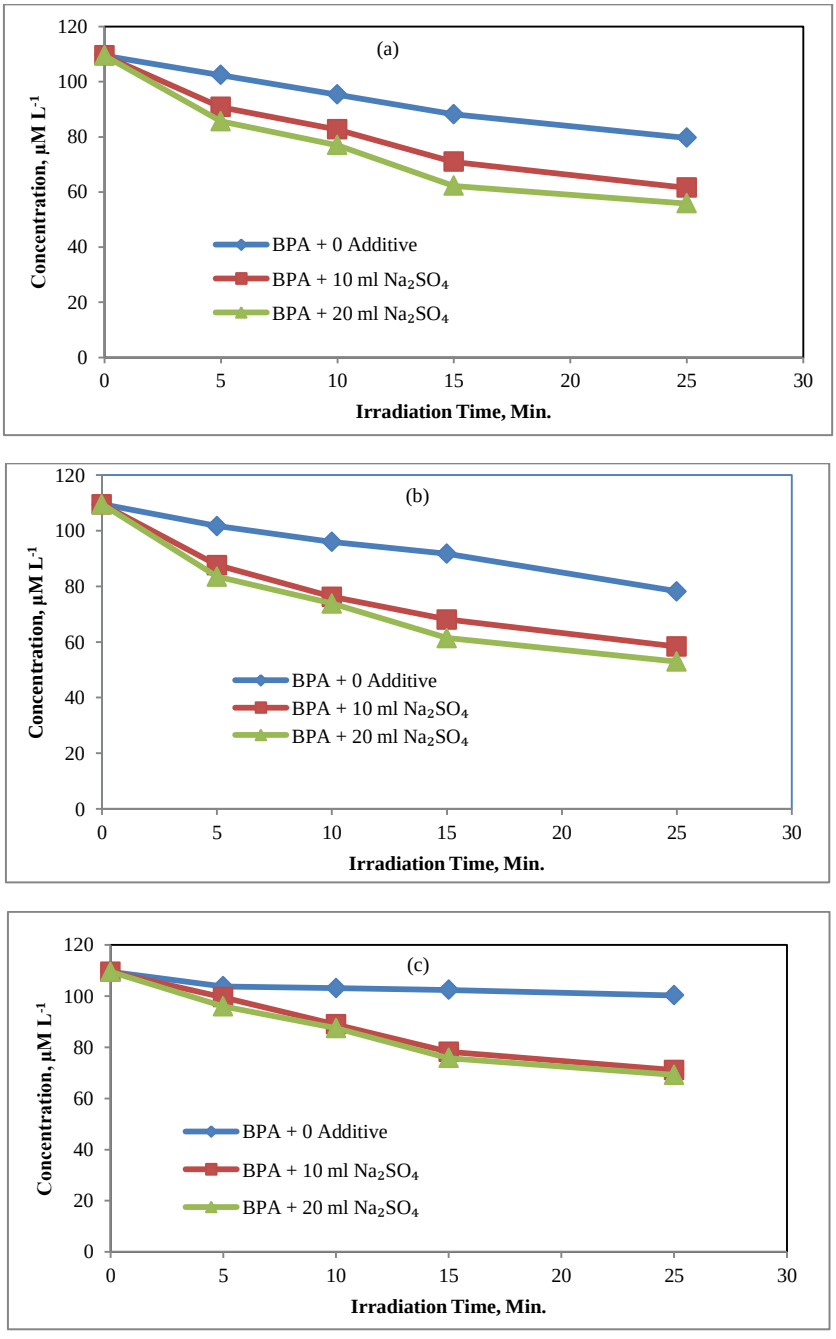

Figure 6. Sonochemical degradation of BPA, BPA with 10mL and 20mL Na_2SO_4 at (a) pH = 6.3 (stock solution), (b) pH = 2, and (c) pH = 8.

The similar trend as figure 8a which means that at pH 2 and 8, the BPA degradation rate is increased for the increasing of the concentrations of Na_2SO_4 as well as the sonication time. It is also found that at an acidic medium(at pH 2) the degradation is much higher than in the other two systems. The process of salt degradation can be described as follows: when salt is added to a solution, molecules from the bulk liquid phase collide

with each other at the bulk-bubble interface [55, 56]. Salts have the potential to raise the aqueous phase's hydrophilicity, ionic strength, and surface tension, and reduce the vapor pressure [55, 56]. These all contribute to the bubbles collapsing more forcefully, which causes a high level of BPA degradation.

Effect of H_2O_2 on BPA degradation

Sonochemical treatment of pure BPA, BPA with 100 µL H_2O_2, and BPA with 200 µL H_2O_2 is done and the obtained data is plotted in figure 7 which indicates that the most efficient dose for BPA degradation is 200 µL H_2O_2 (Figure 7a) for stock solution as well as for solution at pH 2 (Figure 7b) and pH 8 (Figure 7c). Hence the Higher dose of H_2O_2 and higher irradiation time is more effective for BPA degradation in at an acidic medium than a basic medium. A Similar type of BPA degradation improvement studies is carried out by Kim et al. [57]. H_2O_2 increases the BPA degradation by producing the additional OH radical [58].

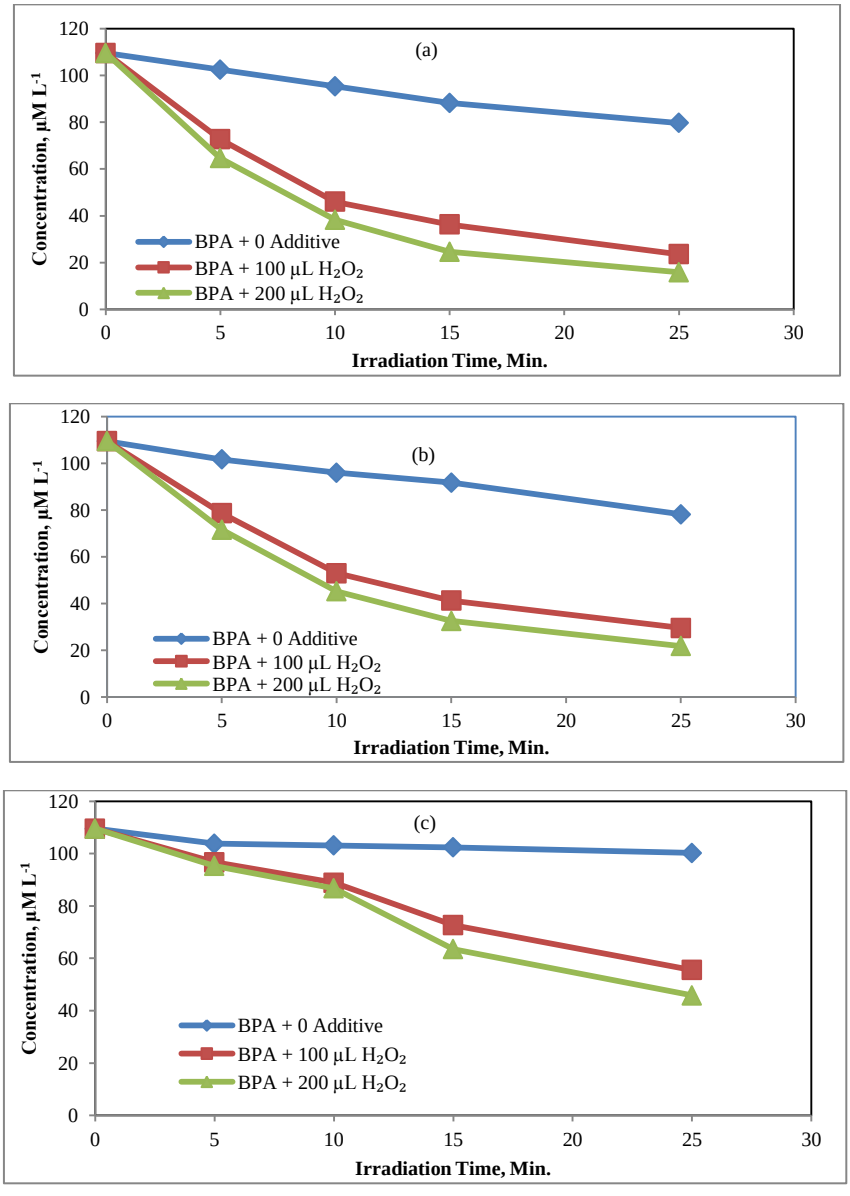

Figure 7. Sonochemical degradation of BPA, BPA with 100 µL and 200 µL H_2O_2 at (a) pH = 6.3 (stock solution), (b) pH = 2, and (c) pH = 8.

Effect of CCl_4 on BPA degradation

CCl_4 of various doses incorporated into BPA and ultrasonic irradiation is done at different pH. The experimental result is summarized in Figure 8 and we found that at pH 2 (Figure 8b) BPA is highly degraded

for the 200 µL CCl_4 dose. At the same time, 200 µL CCl_4 dose shows greater efficiency than 100 µL CCl_4 for BPA degradation at pH 6.3 and 8 (Figure 8a and 8c) which is followed by pure BPA also. Therefore the higher doses and irradiation time favor the degradation of BPA at low pH compared to higher pH. It is thought that the sonolytic breakdown of CCl_4 created chlorine species and radicals, which accelerated the breakdown of BPA. Previous research indicates that the presence of carbon tetrachloride during ultrasonic radiation exposure promotes the development of hydroxyl and hydroperoxyl oxidizing species. Oxidized products arising from the splitting of one aromatic ring, such as mono hydroxylated and dihydroxylated bisphenol A [59, 60], vicinal dicarbonyl and dihydroxy compounds [61], and mono or di-carboxylic compounds [62], are generated during the first fifteen minutes. Gradually, they break down into small-molecule carboxylic acids and other partially oxidized chemicals that can be more or less hazardous, such as 4-iso propane phenol, 4-hydroxyphenyl alcohol, 4-(2Hydroxypropan-2yl)phenol, and 4-propyl benzyl acetaldehyde [63, 64]. Additionally, P-phenyl-p-benzyl-isopropane is produced, which is a reduced and extremely poisonous molecule that needs to be further oxidized [65]. The fact that more products with a more advanced degree of oxidation are generated in a shorter amount of time in the resulting combination of compounds than in the case of ultrasonic exposure without supplementary compounds highlights the beneficial effect of CCl_4.

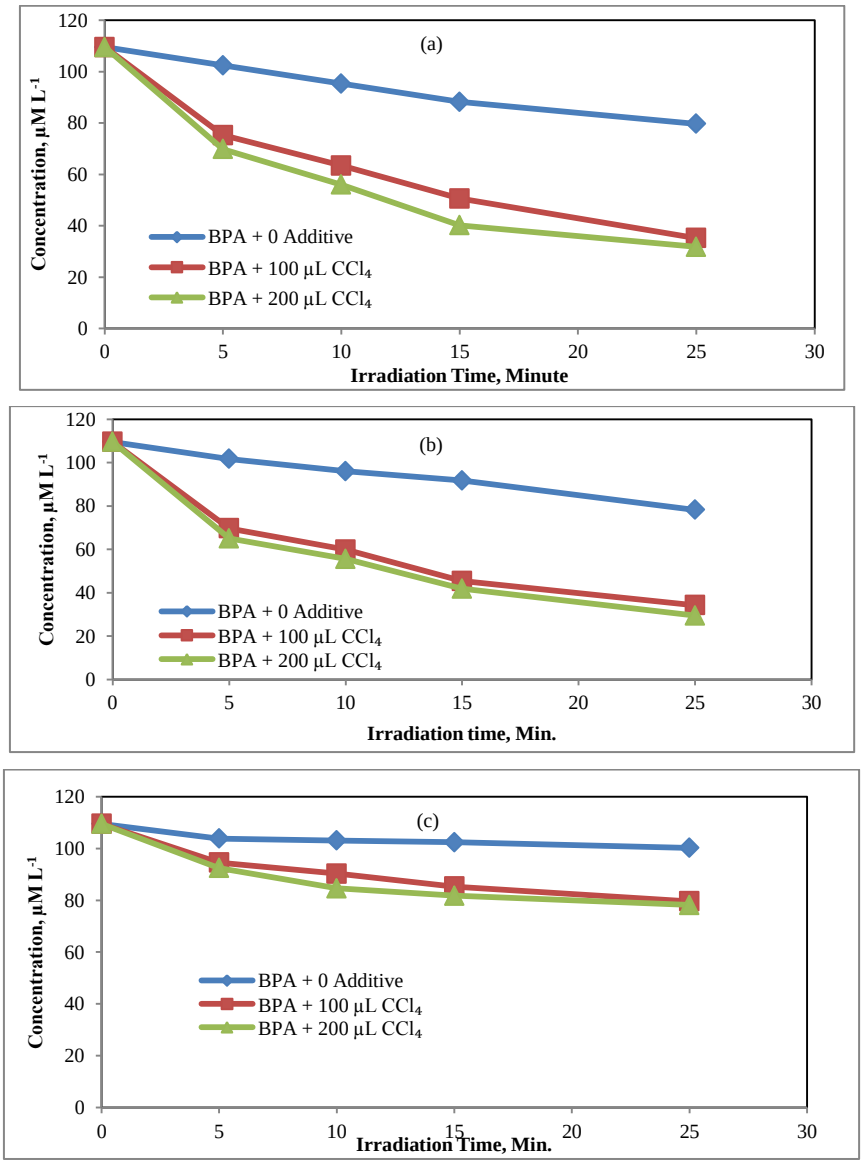

Figure 8. Sonochemical degradation of BPA, BPA with 100 µL and 200 µL CCl_4 at (a) pH = 6.3 (stock solution), (b) pH = 2, and (c) pH = 8.

Maximum degradation of BPA

Figure 9 shows the maximum degradation of BPA in this study and indicates that 200 µL H_2O_2 degrades the highest amount of BPA at pH 6.63(Stock solution).

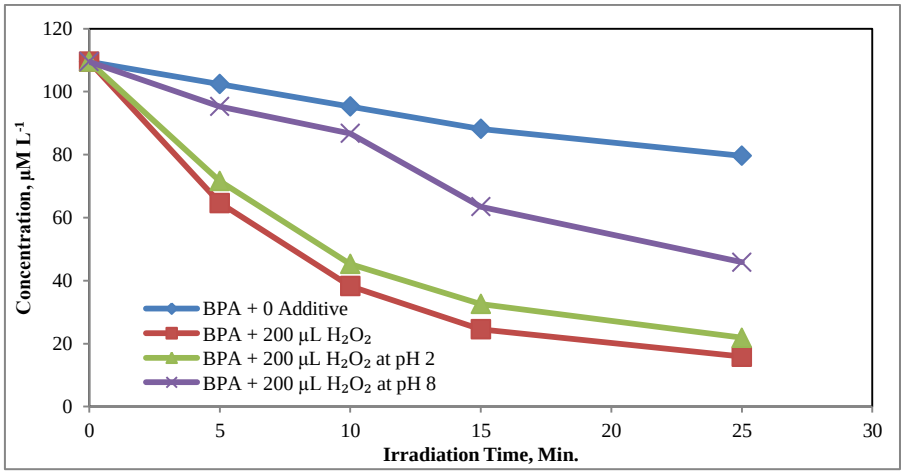

Figure 9. Maximum degradation of BPA at different pH.

CONCLUSIONS

Various parameters, including pH, the addition of ZnO nanoparticle, NaCl, Na_2SO_4, H_2O_2, and CCl_4, were investigated to determine the rate of sonochemical breakdown of BPA. In an acidic medium, BPA degraded more quickly. Utilizing ZnO nanoparticles greatly increased the rate of degradation. However, inorganic salts like NaCl and Na_2SO_4 help to accelerate BPA degradation. Compared to NaCl, Na_2SO_4 has a larger capacity for deterioration. In the presence of H_2O_2, the rate of decomposition is also higher than in pure BPA. In this investigation, the dose of H_2O_2 at 200 µL exhibits the highest degradation rate when compared to the other doses. On the other hand 200 µL CCl_4 degraded BPA more rapidly than 100 µL CCl_4. The results showed that, the maximum BPA degradation was obtained at pH 6.3(stock solution), pH 2, and pH 8 by using 200 µL H_2O_2. The results also confirmed that the BPA degradation rate increases as the order of H_2O_2 > CCL_4 > ZnO > Na_2SO_4 > NaCl in an acidic medium. Therefore, BPA can be degraded by ultrasound in an aqueous media using any of these additives and catalysts.

Conflict of interests

Authors have declared that no conflict of interests exists.

REFERENCES

1. Kitajima M., Hatanaka S.I., Hayashi S., 2006. Mechanism of O_2-accelerated sonolysis of bisphenol A. Ultrasonics. 44, e371- e373.

2. Krishnan A.V., Starhis P., Permuth S.F., Tokes L., Fledman D., 1993. Bisphenol-A: an estrogenic substance is released from polycarbonate flasks during autoclaving. Endocrinol. 132(6), 2279-86.

3. Brostons J.A., Olea- Serrano M.F., Villalobos M., Pedraza V., Olea N., 1995. Xenoestrogens released from lacquer coatings in food cans. Environ. Health Perspect. 103(6), 608-612.

4. Suarez S., Sueiro R.A., Garrido J., 2000. Genotoxicity of the coating lacquer on food cans, bisphenol A diglycidyl ether -BADGE, its hydrolysis products and a chlorohydrin of BADGE. Mutat Res. 470, 221-228.

5. Loganathan B.G., Lam P.K.S. Global Contamination Trends of Persistent Organic Chemicals, 1st ed., CRC Press: USA, 2012. pp. 3-32.

6. González-Mille D.J., Ilizaliturri-Hernández C.A., Espinosa-Reyes G., Cruz-Santiago O., Cuevas-Díaz, M.D.C.; Martín Del Campo C.C., Flores-Ramírez, 2019. R. DNA Damage in different wildlife species exposed to persistent organic pollutants (POPs) from the delta of the Coatzacoalcos Ver, Mexico. Ecotoxicol Environ Saf. 180, 403-411.

7. Ghassabian A., Vandenberg L., Kannan K., Trasande L., 2022. Endocrine-disrupting chemicals and child health. Annu. Rev Pharmacol Toxicol. 62, 573-594.

8. Mahmad A., Zango Z.U., Noh T.U., Usman F., Aldaghiri O.A., Ibnaouf K.H., Shaharun M.S., 2023. Response surface methodology and artificial neural network for prediction and validation of bisphenol a adsorption onto zeolite imidazole framework. Groundw. Sustain Dev. 21, 100925.

9. Preethi S., Sandhya K., Lebonah D.E., Prasad Ch.V., Sreedevi B., Chandrasekhar K., Kumari J.P., 2014. Toxicity of bisphenol a on humans: a review. Int Lett Nat Sci. 27, 32-46.

10. Suresh S., Singh S.A., Vellapandian C., 2022. Bisphenol A exposure links to exacerbation of memory and cognitive impairment: A systematic review of the literature. Neurosci Biobehav Rev. 143, 104939.

11. Roy D., Palagat M., Chen C.W., Thomas R.D., Colerangle J., Atkinson A., Yan Z.J., 1997. Biochemical And Molecular Changes At The Cellular Level In Response To Exposure To Environmental Estrogen-Like Chemicals. J Toxicol and Environ Health. 50(1), 1-30.

12. Matsumoto G., Ishiwatari R., and Hanya T., 1977. Gas chromatographic-mass spectrometric identification of phenols and aromatic acids in river waters. Water Res. 11(8), 693-698.

13. Matsumoto G., 1982, Comparative study on organic constituents in polluted and unpolluted inland aquatic environments—III: Phenols and aromatic acids in polluted and unpolluted waters. Water Res. 16(5), 551-557.

14. Flint E. B., Suslick K. S., 1991. The Temperature of Cavitation. Science. 253(5026), 1397-1399.

15. Suslick K.S., Hammerton D.A., 1986. The Site of Sonochemical Reactions, IEEE Trans. 2(33), 143.

16. Mason T.J., Lorimer J.P., Sonochemistry: Theory, Applications and Uses of Ultrasound in Chemistry, Halsted Press (Wiley): Chichester, U. K., 1988.

17. Adewuyi Y.G., Appaw C., 2002. Sonochemical Oxidation of Carbon Disulfide in Aqueous Solutions: Reaction Kinetics and Pathways. Ind Eng Chem Res. 41(20), 4957-4964.

18. Appaw C., Adewuyi Y.G., 2002. Destruction of carbon disulfide in aqueous solutions by sonochemical oxidation. J Haz Mat. 90(3), 237-249.

19. Ley S.V., Low C.M.R., Ultrasound in Synthesis; Springer-Verlag (Berlin, New York), 1989.

20. Lu Y., Weavers L.K., 2002. Sonochemical desorption and destruction of 4 chlorobiphenyl from synthetic sediments. Environ Sci Technol. 36(2), 232-237.

21. Hua I., Hoffman M. R., 1997. Optimization of Ultrasonic Irradiation as an Advanced Oxidation Technology. Environ Sci Technol. 31(8), 2237-2243.

22. Sun S., Ren Y., Guo F., Zhou Y., Cui M., Ma J., Han Z., Khim J., 2023. Comparison of effects of multiple oxidants with an ultrasonic system under unified system conditions for bisphenol A degradation. Nati Libr Med. 329, 138526.

23. Liu Y.C., Liu X., Zhang G.H., Liu W., Wang J.Q., Wang X., Chen C.L., Wang,Y., Xiang Z., 2023. Performance and mechanism of a novel S-scheme heterojunction sonocatalyst CuS / $BaWO_4$ for degradation of bisphenol A by ultrasonic activation. Environ. Res. 216 (Pt 4), 114720, DOI: 10.1016/j. envres.2022.114720 Preprints (www.preprints.org) | not peer-reviewed |

24. Deggelmann M., N¨opel J.A., Rüdiger F., Paustian D., Braeutigam P., 2022. Hydrodynamic cavitation for micropollutant degradation in water – Correlation of bisphenol A degradation with fluid mechanical properties. Ultrason Sonochem. 83, 105950.

25. Li X., Zhang Y., Xie Y., Zeng Y., Li P., Xie T., Wang Y., 2018, Ultrasonic-enhanced Fenton-like degradation of bisphenol A using a bio-synthesized schwertmannite catalyst. J Hazard Mater. 344, 689–697.

26. Entezari M.H., Petrier C., Devidal P., 2003. Sonochemical degradation of phenol in water: a comparison of classical equipment with a new cylindrical reactor. Ultrason. Sonochem. 10, 103–108.

27. Okitsu K., Iwasaki K., Yobiko Y., Bandow H., Nishimura R., Maeda Y., 2005. Sonochemical degradation of azo dyes in aqueous solutions: a new heterogeneous kinetics model taking into account the local concentration of OH radicals and azo dyes. Ultrason Sonochem. 12, 255–262.

28. Inoue M., Okada F., Sakurai A., Sakakibara M., 2006. A new development of dyestuffs degradation system using ultrasound. Ultrason Sonochem.13, 313–320.

29. Merouani S., Hamdaoui O., Saoudi F., Chiha M., 2010. Sonochemical degradation of Rhodamine B in aqueous phase: effects of additives. Chem Eng J. 158, 550–557.

30. Kobayashi D., Honma C., Suzuki A., Takahashi T., Matsumoto H., Kuroda C., Otake K., Shono A., 2012. Comparison of ultrasonic degradation rates constants of methylene blue at 22.8 kHz, 127 kHz, and 490 kHz. Ultrason Sonochem. 19, 745–749.

31. Kobayashi D., Honma C., Matsumoto H., Takahashi T., Kuroda C., Otake K., Shono A., 2014. Kinetics analysis for development of a rate constant estimation model for ultrasonic degradation reaction of methylene blue. Ultrason Sonochem. 21, 1489–1495.

32. Kruus P., Burk R.C., Entezari M.H., Otson R., 1997. Sonication of aqueous solutions of chlorobenzene. Ultrason. Sonochem.4, 229–233.

33. Petrier C., Francony A., 1997. Ultrasonic waste-water treatment: incidence of ultrasonic frequency on the rate of phenol and carbon tetrachloride degradation. Ultrason. Sonochem. 4, 295–300.

34. Sponza D.T., Oztekin R., 2014. Dephenolization, dearomatization and detoxification of olive mill wastewater with sonication combined with additives and radical scavengers. Ultrason Sonochem. 21(3), 1244–1257.

35. Zheng W., Maurin M., M.A. Tarr M.A., 2005. Enhancement of sonochemical degradation of phenol using hydrogen atom scavengers. Ultrason Sonochem. 12(4), 313–317.

36. Shirajum M., Ashifuzzaman, M. I., Jahangir H., Kenji O., Hafizur R., Shaharul I., Helal U., 2022. Effects of Additives on Sonolytic Degradation of Azo Dye Molecules Found in Industrial Wastewater. Jurnal Kejuruteraan. 34(1), 41-50.

37. Monjurul I., Saifur Rahman B.M., Most Shahida Kh., Jahangir H., Tanjirul H., Shaharul I, Arifuzzaman Khan G. M., Helal U., 2018. Sonochemical degradation of phenol and Para-Chlorophenol in an Ultrasonic bath in the presence of inorganic salts and H_2O_2. International Journal for Excogitation Education and Research. 1(1), 22-33.

38. Jahangir H., Shirajum M., M. Sh., Samiul B. A., Shaharul I., Marjia Kh., Abdur Razzaque S.M., Helal U., 2023. Effect of Additives on Decomposition of Methyl Orange and Congo Red Dyes Found in Industrial Wastewater. Asian Journal of Physical and Chemical Sciences. 11(3), 52-63.

39. Nagpal M., Kakkar R., 2019. Use of metal oxides for the adsorptive removal of toxic organic pollutants. Sep Purif Technol. 211, 522–539.

40. Wawrzkiewicz M., Wi´sniewska M., Wołowicz A., Gun'ko V.M., Zarko V.I., 2017. Mixed silica-alumina oxide as sorbent for dyes and metal ions removal from aqueous solutions and wastewaters. Microporous Mesoporous Mater. 25, 128–147.

41. Danish M.S.S., Bhattacharya A., Stepanova D., Mikhaylov A., Grilli M.L., Khosravy M., Senjyu T., 2020. A Systematic Review of Metal Oxide Applications for Energy and Environmental Sustainability. Metals. 10, 1604.

42. Huang Y., Su W., Wang R., Zhao T., 2019. Removal of typical industrial gaseous pollutants: From carbon, zeolite, and metal-organic frameworks to molecularly imprinted adsorbents. Aerosol Air Qual Res. 19, 2130–2150.

43. Lee K.M., Lai C.W., Ngai K.S., Juan J.C., 2016. Recent developments of zinc oxide based photocatalyst in water treatment technology: A review. Water Res. 88, 428–448.

44. Hashimoto K., Irie H., Fujishima A., 2005. TiO_2 photocatalysis: A historical overview and future prospects. Jpn J Appl Phys. 44, 8269–8285.

45. Dastan D., Panahi S.L., Chaure N.B., 2016. Characterization of titania thin films grown by dip-coating technique. J Mater Sci Mater Electron. 27, 12291–12296.

46. Dastan D., Panahi S.L., Yengantiwar A.P., Banpurkar A.G., 2016. Morphological and electrical studies of titania powder and films grown by aqueous solution method. Adv Sci Lett. 22, 950–953.

47. Dastan D., 2017, Effect of preparation methods on the properties of titania nanoparticles: Solvothermal versus sol-gel. Appl Phys. A, 1–13, 123–699.

48. Azmina M.S., Nor R.M., Rafaie H.A., Razak N.S.A., Sani S.F.A., Osman Z., 2017. Enhanced photocatalytic activity of ZnO nanoparticles grown on porous silica microparticles. Appl Nanosci. 7, 885–892.

49. Hariharan C., 2006, Photocatalytic degradation of organic contaminants in water by ZnO nanoparticles: Revisited. Appl Catal A Gen. 304, 55–61.

50. Zhaobing G., Qiongyuan D., Duliang H., Chaozhi Zh. , 2012, Gamma radiation for treatment of bisphenol A solution in presence of different additives. Chemical

Engineering Journal. 183, 10–14.

51. Bekkouche S., Bouhelassa M., Hadj Salah N., Meghlaoui F.Z., 2004. Study of adsorption of phenol on titanium oxide (TiO_2). Desalination. 166, 355-362.

52. Sin J.C., Lam S.M., Lee K.T., Mohamed A.R., 2013. Photocatalytic performance of novel samarium-doped spherical-like ZnO hierarchical nanostructures under visible light irradiation for 2,4-dichlorophenol degradation. J Colloid Interf Sci. 401, 40–49.

53. Kamaraj M., Nithya T.G., Chidambararajan P., Muluken Kebede, 2020, Photocatalytic degradation of Bisphenol-A in water under sunlight irradiation over ZnO nanoparticles fabricated by Ethiopian cactus pear fruit peel infusions, Optik - International Journal for Light and Electron Optics. 208, 164539.

54. Mukimin A., Wijaya K., Kuncaka A., 2012. Oxidation ofremazolbrilliant bluer (RB.19) with in situ electro-generated activechlorine using Ti/PbO_2 electrode. Sep Purif Technol. 95, 1−9.

55. Fındık S., Gündüz G., 2007. Sonolytic degradation of acetic acid in aqueous solutions. Ultrasonics Sonochemistry. 14(2), 157-162.

56. Seymour J.D., Gupta, R.B. 1997. Oxidation of aqueous pollutants using ultrasound: salt-induced enhancement. Industrial & Engineering Chemistry Research. 36(9), 3453-3457.

57. Kim I., Hong S., Hwang I., Kwon D., Kwon J, Huang C.P., 2007. TOC and THMFP reduction by ultrasonic irradiation in waste water effluent. Desalination. 202(1-3), 9–15.

58. Gogate P.R., Pandit A.B 2004. A review of imperative technologies for wasterwater treatment II: hybrid methods. Advances in Environmental Research. 8(3-4), 553–597.

59. Zühlke M.K., Schlüter R., Mikolasch A., Henning A.K., Giersberg M., Lalk M., Kunze G., Schweder T., Urich T., Schauer F., 2020. Biotransformation of bisphenol A analogues by the biphenyl-degrading bacterium Cupriavidus basilensis - a structure-biotransformation relationship. Appl Microbiol Biotechnol. 104, 3569–3583

60. Stack D.E., Mahmud B., 2018. Efficient access to bisphenol A metabolites: Synthesis of monocatechol, mono-oquinone, dicatechol, and di-o-quinone of bisphenol A. Synt Commun. 48(2), 161–167.

61. Wua Q., Fanga J., Li S., Wei J., Yanga Z., Zhaoa H., Zhaoa C., Cai Z., 2017. Interaction of bisphenol A 3,4-quinone metabolite with glutathione and ribonucleosides/deoxyribonucleosides *in vitro*. J HazMat. Part A. 323, 195-202.

62. Deborde M., Rabouana S., Mazellier P., Duguet J.P., Legube B., 2008. Oxidation of bisphenol A by ozone in aqueous solution. Water Res. 42, 4299–4308.

63. Widhiastuti F., Fan L., Paz-Ferreiro J., Chiang K., 2022. Oxidative treatment of bisphenol A by Fe(VI) and Fe(VI)/H_2O_2 and identification of the degradation products. Environ Technol Innov. 28, 102643.

64. Gao C., Zeng Y.H.; Li C.Y., Li L., Cai Z.H., Zhou J., 2021. Bisphenol A biodegradation by Sphingonomas sp. YK5 is regulated by acyl-homoserine lactone signaling molecules. Sci Total Environ. 802, 1-8.

65. Yue W., Yin C.F., Sun L., Zhang J., Xu Y., Zhou N.I., 2021. Biodegradation of bisphenol A polycarbonate plastic by Pseudoxanthomonas sp. Strain NyZ600. J Haz Mat. 416, 1-11.